

# Multifunctional Amino-Decorated Metal-Organic Frameworks: Nonlinear-Optic, Ferroelectric, Fluorescence Sensing and Photocatalytic Properties

Lili Wen,<sup>\*a</sup> Li Zhou,<sup>a</sup> Bingguang Zhang,<sup>b</sup> Xianggao Meng,<sup>a</sup> Hua Qu,<sup>a</sup> and Dongfeng Li<sup>\*a</sup>

<sup>a</sup>Key Laboratory of Pesticide & Chemical Biology of Ministry of Education, College of Chemistry,  
Central China Normal University, Wuhan, 430079, P. R. China

<sup>b</sup>Key Laboratory of Catalysis and Materials Science of the State Ethnic Affairs Commission & Ministry  
of Education, South-Central University for Nationalities, Wuhan 430074, P. R. China

Fax: (+)86 27 67867232

E-mail: [wenlili@mail.ccnu.edu.cn](mailto:wenlili@mail.ccnu.edu.cn) (L. Wen), [dfli@ccnu.edu.cn](mailto:dfli@ccnu.edu.cn) (D. Li)

**Table S1** Selected bond lengths (Å) and bond angles (deg) for 1–4

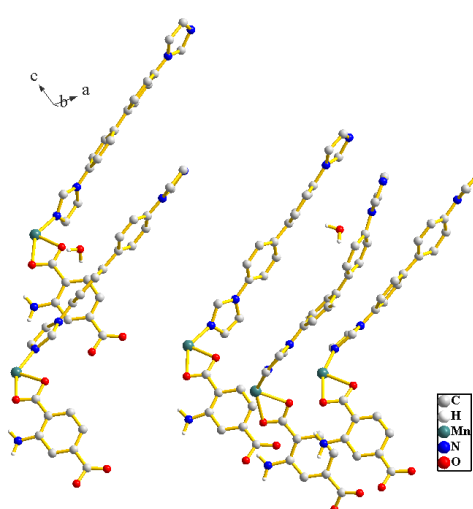
1 <sup>a</sup>						
Mn1–O1	2.209(4)	Mn1–O2	2.317(3)	Mn1–N2	2.085(4)	Mn1–O3#1
Mn1–N5#2	2.060(5)	Mn2–N10#4	2.102(4)	Mn2–O8#3	2.376(3)	Mn2–O6
Mn2–O5	2.225(3)	Mn2–O7#3	2.156(3)	Mn3–O12#1	2.222(3)	Mn3–O11#1
Mn3–N12	2.201(4)	Mn3–O9	2.091(3)	Mn3–O10	2.338(3)	Mn4–O13
Mn4–O15#1	2.175(3)	Mn4–N17	2.162(4)	Mn4–O16#1	2.480(3)	Mn4–O14
Mn5–O19#7	2.316(3)	Mn5–N22	2.134(4)	Mn5–O18	2.361(3)	Mn5–O20#7
O4#1–Mn1–N5#2	140.02(15)	N2–Mn1–N5#2	100.19(17)	O1–Mn1–O3#1	147.46(13)	O6–Mn2–O8#3
N7–Mn2–N10#4	106.66(15)	O9–Mn3–O11#1	143.16(12)	N12–Mn3–N15#5	85.15(14)	O10–Mn3–O12#1
O14–Mn4–O16#1	108.94(11)	N17–Mn4–N20#6	89.32(14)	O17–Mn5–O19#7	138.95(12)	O18–Mn5–O20#7
Zn1–O2	1.967(6)	Zn1–N1	1.950(7)	Zn1–N3#1	1.905(7)	Zn1–O3#2
O3#2–Zn1–N1	112.9(3)					
2 <sup>b</sup>						
Co1–O2	1.954(5)	Co1–N2	1.988(6)	Co1–N5#1	2.028(6)	Co1–O3#2
O2–Co1–N5#1	110.1(2)					
3 <sup>c</sup>						
Co1–O1	2.234(2)	Co1–O2	2.074(2)	Co1–N2	2.098(2)	Co1–N3#1
O4#2–Co1–N2	105.87(9)	O1–Co1–N3#1	93.07(9)	O2–Co1–N3#1	105.83(10)	
4 <sup>d</sup>						
Co1–O1						
O4#2–Co1–N2						

<sup>a</sup>Symmetry codes for **1**: #1 x, -y, 1/2+z; #2 -1/2+x, 1/2-y, -1/2+z; #3 x, 1-y, 1/2+z; #4 -1/2+x, 1/2-y, -1/2+z; #5 -1/2+x, 1/2-y, -1/2+z; #6 -1/2+x, 1/2-y, -1/2+z; #7 x, 1-y, 1/2+z; #8 -1/2+x, 3/2-y, -1/2+z

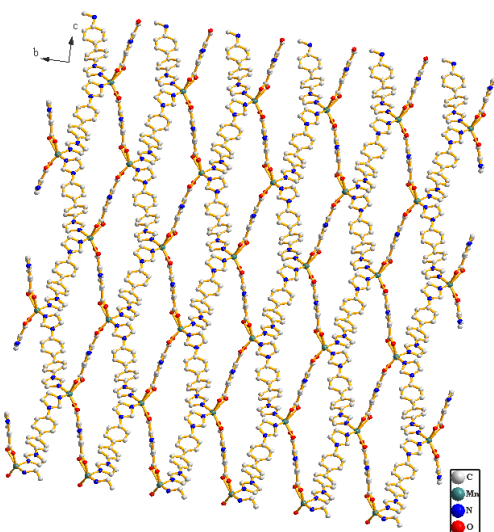
<sup>b</sup>Symmetry codes for **2**: #1 x, 2-y, -1/2+z; #2 1/2+x, 1/2-y, 1/2+z

<sup>c</sup>Symmetry codes for **3**: #1 x, -y, -1/2+z; #2 -1/2+x, 3/2-y, -1/2+z

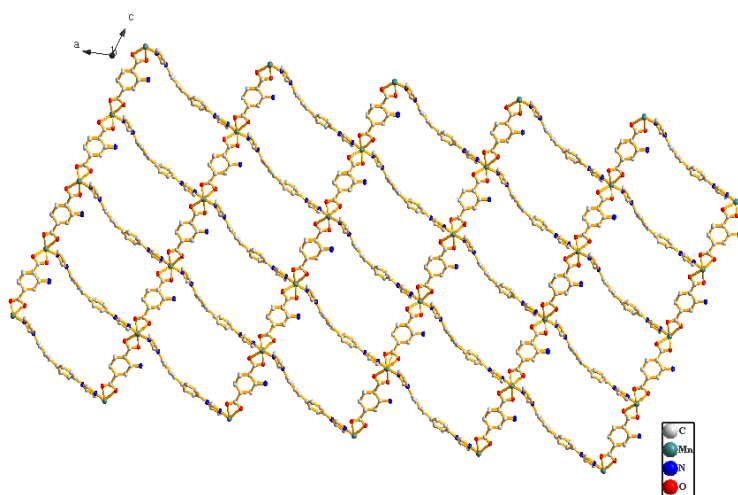
<sup>d</sup>Symmetry codes for **4**: #1 -1+x, y, z; #2 x, 1/2-y, -1/2+z

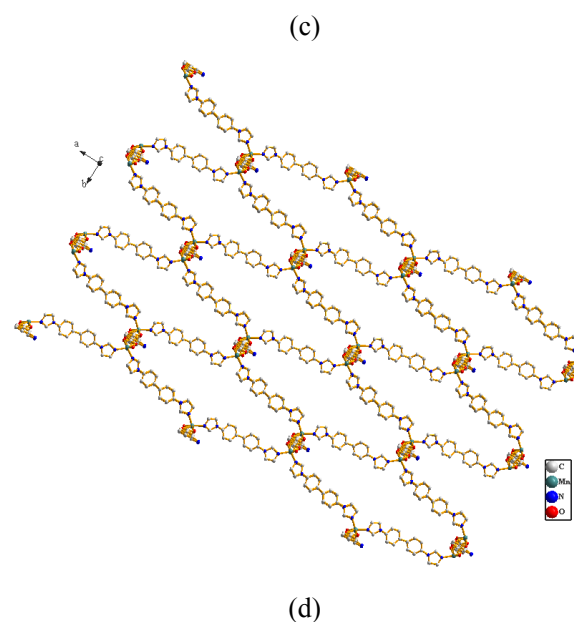


(a)



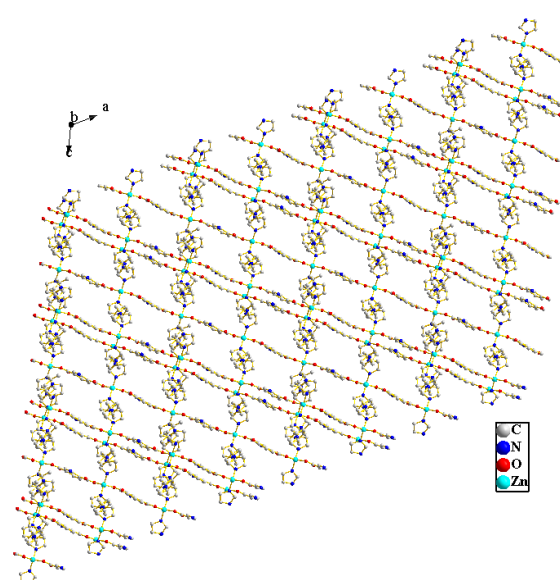
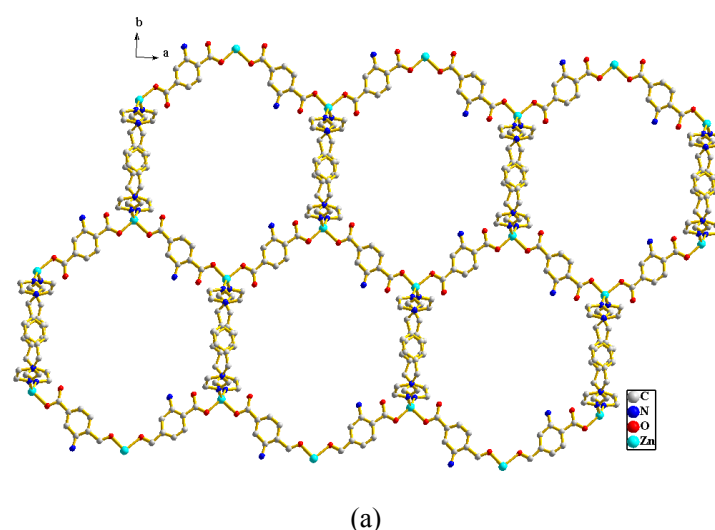
(b)





(d)

**Fig S1.** The asymmetric unit in **1** (a); View of the 3D single framework of **1** along *a* (b), *b* (c) and *c* (d) axes.



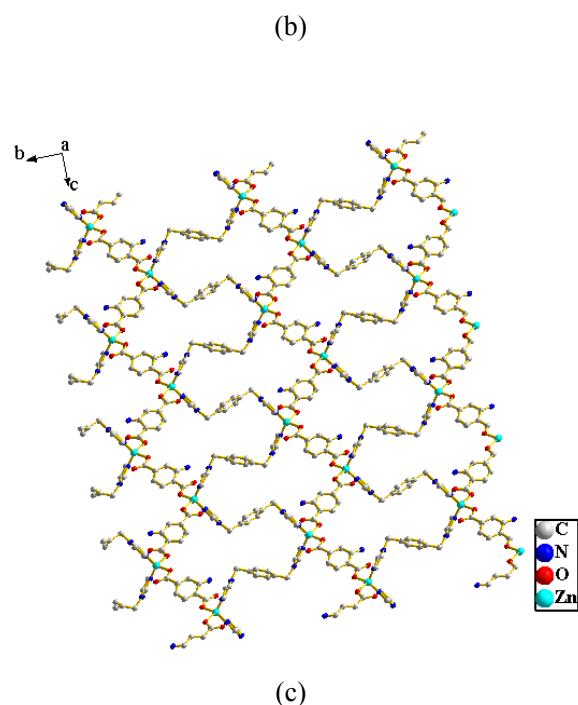


**Fig. S2** View of the 3D single framework of **2** along the *c* (a), *b* (b) and *a* (c) axes.

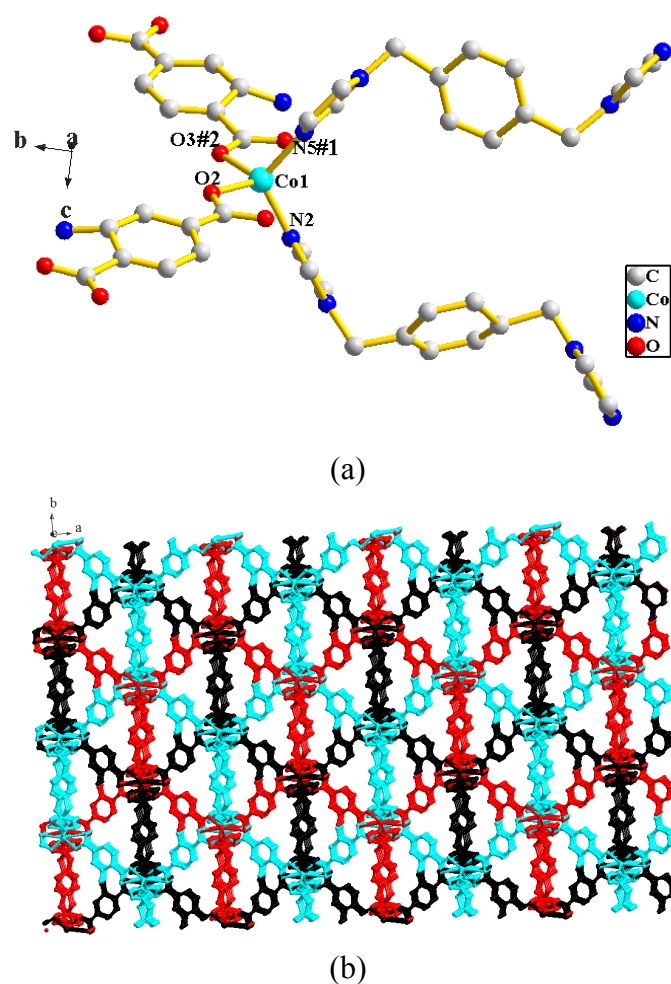


**Fig. S3** (a) Coordination environments of Co atoms with hydrogen atoms omitted for clarity and (b)

view of the 3-fold interpenetrating for **3**.

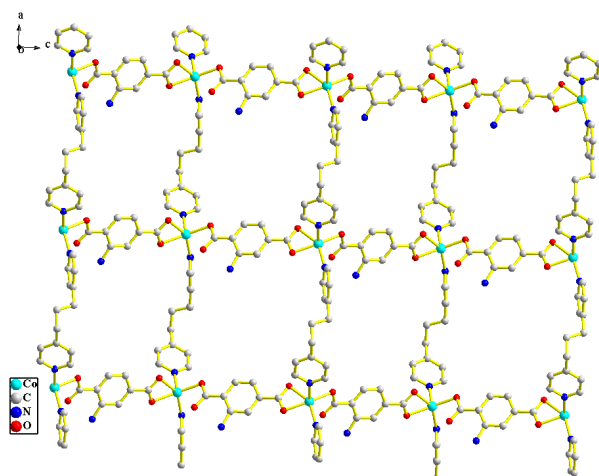


**Fig. S4** View of the 2D framework of **4** along the *b* axis.

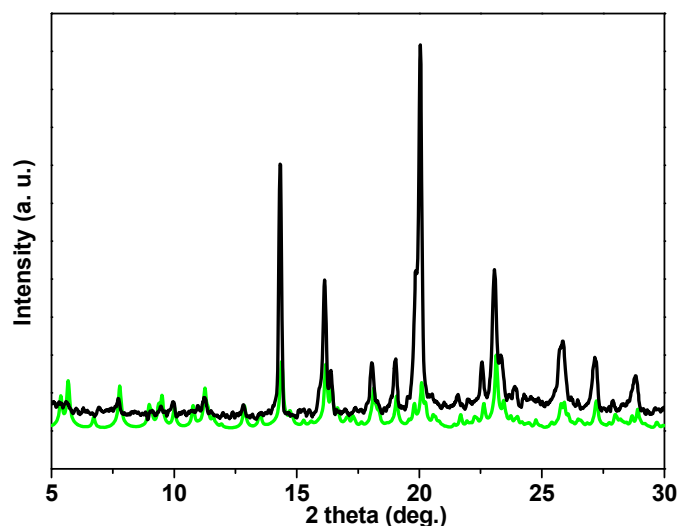


**Fig. S5** X-ray power diffraction diagram of the simulated spectra from single crystal data of **1** (green), compound **1** (black).

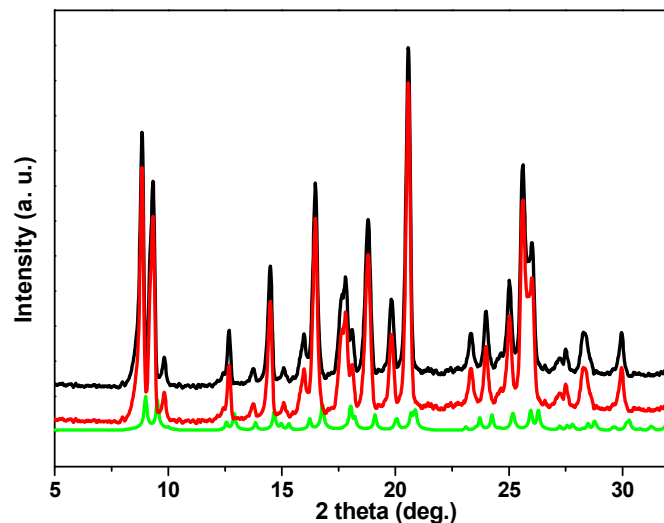


**Fig. S6.** X-ray power diffraction diagram of the simulated spectra from single crystal data of **2** (green), compound **2** (red), **2** after photocatalysis process (black).

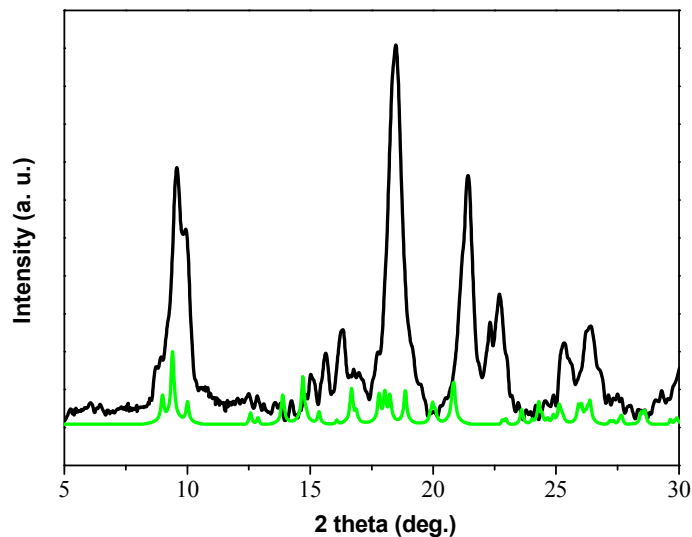


**Fig. S7.** X-ray power diffraction diagram of the simulated spectra from single crystal data of **3** (green), compound **3** (black).

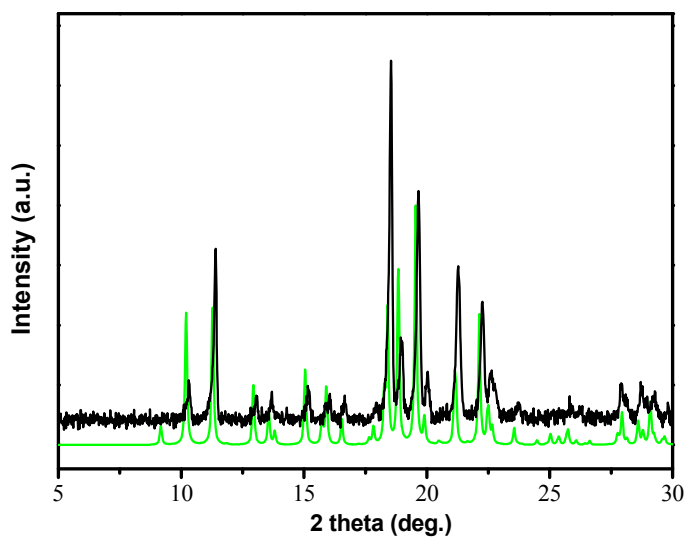


**Fig. S8.** X-ray power diffraction diagram of the simulated spectra from single crystal data of **4** (green), compound **4** (black).

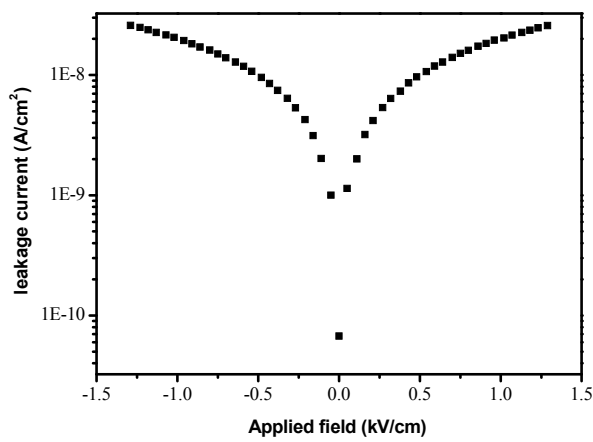


**Fig. S9** Leakage currents *versus* electric fields for **1**.

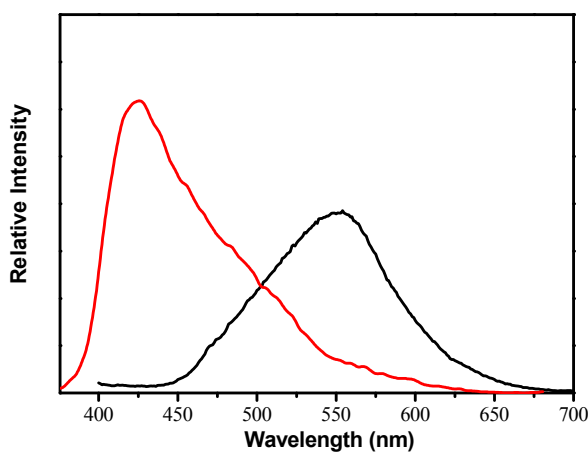


**Fig. S10** Fluorescent emission spectra of complex **2** (red) and free ligand  $\text{NH}_2\text{bdcH}_2$  (black) in solid

state at room temperature, excited at 380 nm.

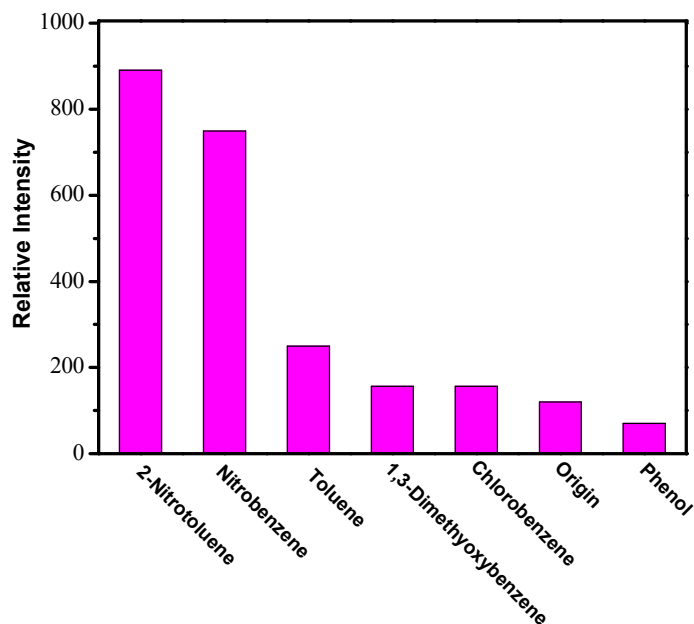


**Fig. S11** Comparison of the solid state luminescence intensity of **2** introduced into different analytes (0.2 mL) in CH<sub>3</sub>OH solutions (20 mL).

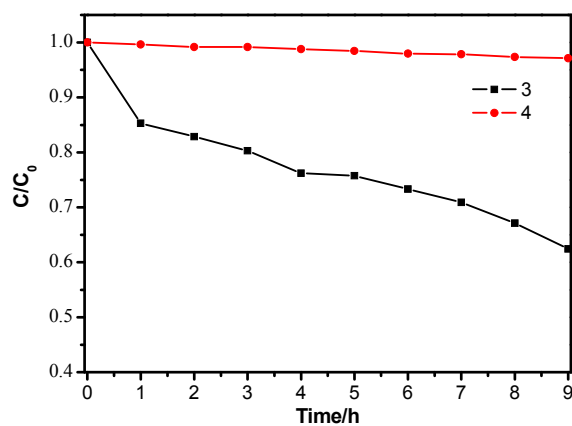
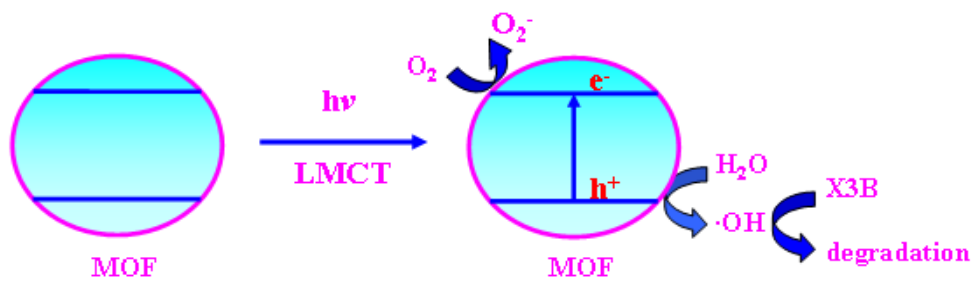


**Fig. S12.** Degradation profiles for X3B in the presence of compounds **3** or **4** under visible light.

### Possible photocatalytic reaction mechanism

Because the HOMO is mainly contributed by oxygen and (or) nitrogen 2p bonding orbitals (valence band, VB) and the LUMO by empty transition metal orbitals (conduction band, CB). Under visible light irradiation, electrons ( $e^-$ ) in the HOMO (VB) of MOF were excited to its LUMO (CB), with same amount of holes ( $h^+$ ) left in VB. The HOMO strongly demands one electron to return to its stable state. Therefore, one electron was captured from water molecules, which was oxygenated into ·OH active

species. Meanwhile, the electrons ( $e^-$ ) in LUMO could be combined with the oxygen adsorbed on the surfaces of MOF to form  $\cdot O_2^-$ , then they might transform to the hydroxyl radicals ( $\cdot OH$ ). Then the formed  $\cdot OH$  radicals could cleave X3B effectively to complete the photocatalytic process.



**Scheme S1.** A simplified model to illustrate the photocatalytic degradation mechanism of X3B on catalyst 5.

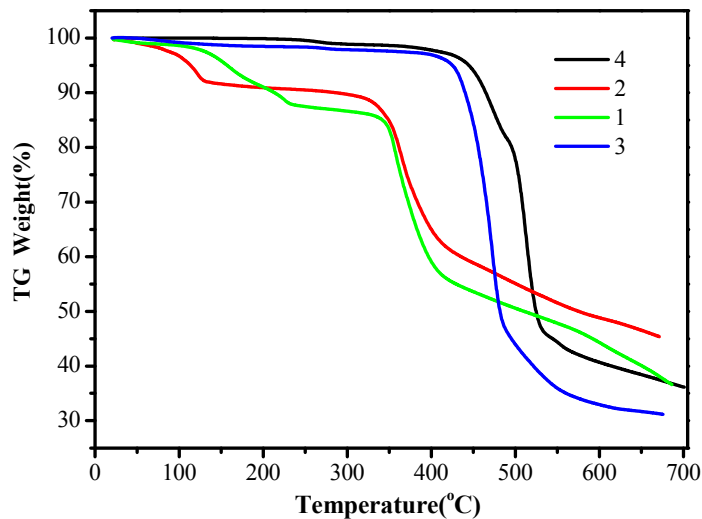


**Fig. S13** TG curves of compounds 1-4.